

SPARE UNDULATOR PRODUCTION FOR PAL-XFEL HX1 BEAMLINE

Jang-Hui Han*, Sojeong Lee, Young Gyu Jung, Dong-Eon Kim,
 Pohang Accelerator Laboratory, Pohang, Korea

Abstract

In the PAL-XFEL hard X-ray beamline, 20 undulator segments with a 26 mm period and a 5 m length are installed and operated for XFEL user service. One spare undulator was manufactured in December 2018. The magnetic measurements and tuning was carried out recently. We report the magnet block sorting, the magnetic measurements and the tuning results.

INTRODUCTION

Pohang Accelerator Laboratory X-ray Free Electron Laser (PAL-XFEL) is operational for users since 2017 [1, 2]. PAL-XFEL has two undulator beamlines, one hard X-ray and one soft X-ray. The hard X-ray undulator line is placed at the end of the main linac, where an electron beam is accelerated up to 10 GeV. The soft X-ray line is branched at the 3 GeV point of the main linac and further accelerated up to 3.15 GeV.

The hard X-ray beamline has twenty undulator segments. The undulator is a hybrid type with NdFeB magnets and Vanadium Permendur poles. The period is 26 mm and the segment length is 5 m. The magnet gap is 8.3 mm. At the minimum gap, the effective flux density is 0.812 T and the deflecting parameter K is 1.973. The undulators for the soft X-ray line are similar the hard X-ray ones except for the period, 35 mm [3].

In 2018, a new hard X-ray undulator was built by refurbishing the mechanical frame and control system of a prototype undulator. The prototype undulator was originally constructed in the very early stage of the PAL-XFEL project. The undulator period was different from the present hard or soft X-ray undulators. Even though the magnet structure could not be re-used, the frame was reused for this spare one. During 2020 summer maintenance, this new undulator will be installed upstream of the first undulator segment of the hard X-ray beamline.

MAGNET BLOCK SORTING

The magnetic field through an undulator segment should be as uniform as a tens thousandth to make the phase error within a few degrees. Field errors of the magnet blocks for this undulator production are in one percent range (Fig. 1).

The permanent magnet block has a “hot and cold side effect”. This effect is caused by the magnet block manufacturing process. The magnetization vector of a magnet block has not only M_z component, but also minor M_x and M_y components [4]. Due to the imperfection of magnetization, there is a difference in the B_z field strength between top and bottom sides. The information of the measured magnetic field and moment of the magnet blocks were supplied by

* janghui_han@postech.ac.kr

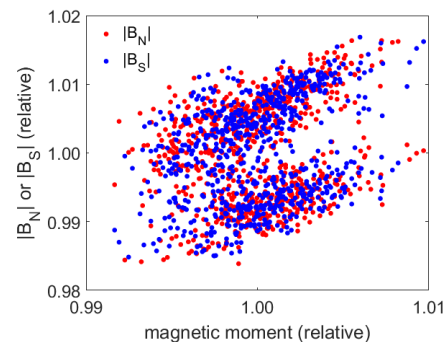


Figure 1: Magnetic field distribution of magnet blocks to magnetic moments.

the vendor. The field of the blocks was measured at a few centimeters from the face.

Figure 2 shows the possible pole field when magnet blocks are distributed randomly. The dotted lines at the middle show the median values of $|B_N|$ and $|B_S|$. The pole fields are placed within about 1%, however a significant pole tuning should be carried out to satisfy the phase error requirement.

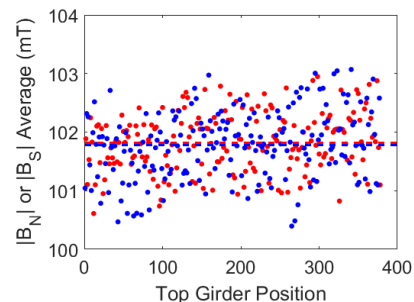


Figure 2: Pole field distribution for randomly installed magnet blocks. The horizontal axis is the pole number in the top magnet structure.

To achieve a field uniformity through an undulator segment, the magnet blocks were sorted and arranged to minimize the field difference among poles as shown in Fig. 3. First, all the magnet blocks were ordered by the $|B_N|$ and $|B_S|$. Then, the magnet block with the median value of $|B_N|$ (or $|B_S|$) is selected to be placed at the first place where an end of the top or bottom magnet structure. In Fig. 3, the block is M1 and the field is $B_{1z}(s)$. Even though the magnetic field to the end direction (left direction here) is close to the median value, the field of the other side (right direction) of the magnet block ($B_{1z}(N)$) in Fig. 3) can be far from the median value. After placing a pole (P1), a pair magnet block (M3) is chosen so that the field at the pole is averaged by the

Content from this work may be used under the terms of the CC BY 3.0 licence (© 2019). Any distribution of this work must maintain attribution to the author(s), title of the work, publisher, and DOI

field ($B_{3z}(N)$) of the block. Such procedures are repeated till the other end of the magnet structure.

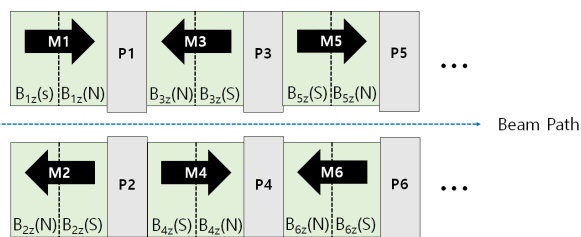


Figure 3: Magnet block pairing.

After paring the magnet blocks, the pole field was calculated again as shown in Fig. 4. By simple paring, the pole field can become uniform. Note that enough spare magnet blocks are necessary for this pairing procedure. Field distribution within a magnet block are ignored in this model. Nevertheless, this simple magnet paring would be a good start of pole tuning for a new undulator segment.

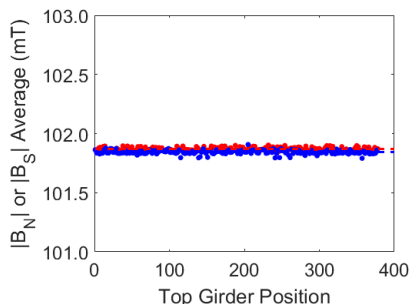


Figure 4: Calculated pole field distribution for magnet blocks sorted by magnetic field pairing.

FIRST MEASUREMENTS

The assembled undulator was measured with a Hall probe. Three FW Bell GH-700 Hall sensors were used for the 3D field measurement. The minimum gap of the magnet structure is 8.3 mm and the tuning gap is 9.5 mm. The vertical field centers of the poles were measured at the 9.5 mm tuning gap as shown in Fig. 5. The colors in the figure displays different magnet structures. The deviation is within $\pm 30 \mu\text{m}$, but there is a drift between magnet structures.

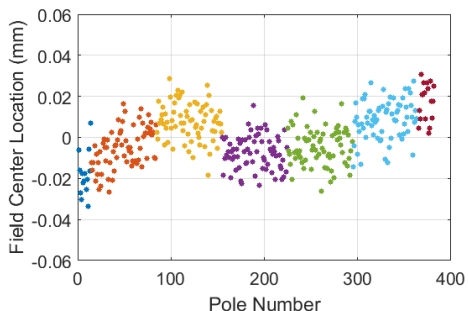


Figure 5: Vertical pole field centers before tuning.

The half gap, the height to be corrected for both top and bottom poles to get an ideal field profile, is plotted in Fig. 6. The four poles near the end are not shown in the figure because the deviations are larger than 0.2 mm. The pole heights in the figure show a drift with linear and quadratic components through the magnet structures.

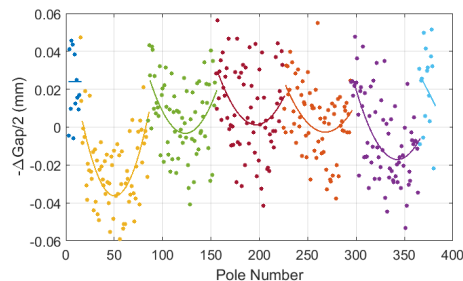


Figure 6: Pole height deviation from ideal position at 9.5 mm gap before tuning. Quadratic fits are applied for each magnet structure.

From the measurements in Fig. 6, a possible magnet structure deformation was estimated as in Fig. 7. The 0.9 m long magnet structures (M1 ~ M5) are fixed to the top or bottom girders. This deformation is larger for narrower gaps.

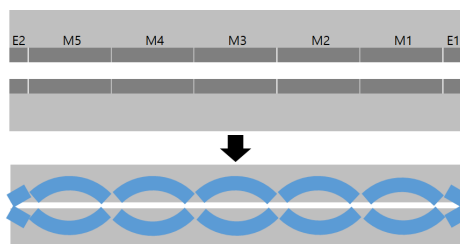


Figure 7: Magnet structure deformation estimated from field measurement.

The phase error distribution before pole tuning is shown in Fig. 8. The short range deviation is small, but there is a long range drift over 80 degree. The rms phase error is 21° .

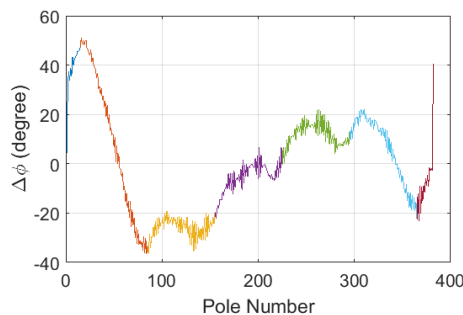


Figure 8: Phase error measured at 9.5 mm gap before tuning.

The poles are assembled to the magnet structure with an accuracy of a few micrometer to the upper face of the structure. The face was carefully machine to have a few tens micrometer flatness, but such a surface roughness can already affect the phase error.

POLE TUNING

The hight and roll angle of a pole can be adjusted with four screws independently. The pole tuning was carried out with six times iteration. The vertical pole field center deviation measured at the 9.5 mm gap is shown in Fig. 9.

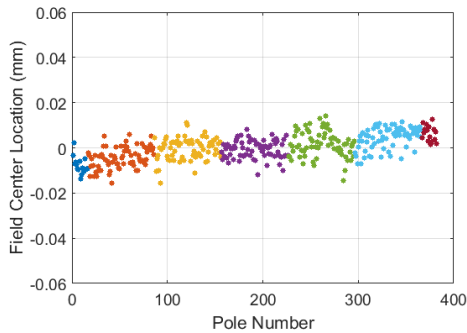


Figure 9: Vertical pole field centers after tuning.

The large long range drift as well as the short range deviation of the pole heights was corrected (Fig. 10). The standard deviation of the pole heights is $2.3 \mu\text{m}$

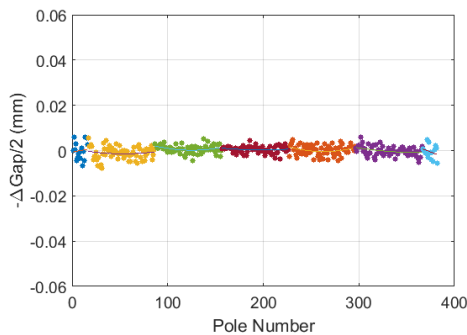


Figure 10: Pole height deviation from ideal position at 9.5 mm gap after tuning.

The phase error distribution before pole tuning is shown in Fig. 11. The rms phase error is 1.78° . The phase er-

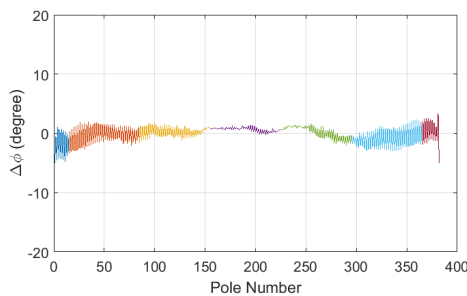


Figure 11: Phase error measured at 9.5 mm gap after tuning.

rors for the operational gaps were measured and plotted in Fig. 12. The black dots are measurements without background field compensation. The red dots are measurements in the magnetic environment where the undulator is to be installed (HX104). The background field in the location in the PAL-XFEL hard X-ray tunnel were measured with a

fluxmeter. The same field was configured with two sets of large Helmholtz coils in the measurement lab. The measured undulator deflection parameters, K , for the operational gaps are shown in Fig. 13.

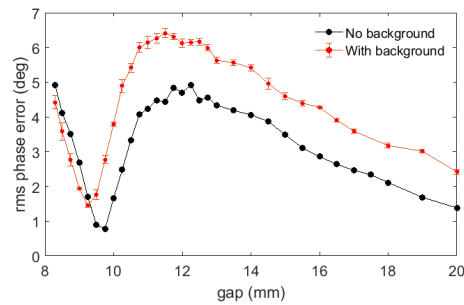


Figure 12: Phase error for various gaps after tuning.

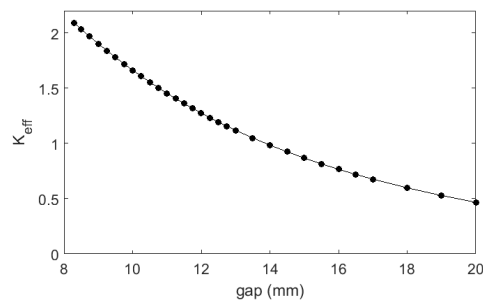


Figure 13: K parameters measured for various gaps.

The entrance and exit kicks for horizontal (x) and vertical (z) directions were analyzed from the measurements and plotted in Fig. 14. The requirement is within 1.5 Gm .

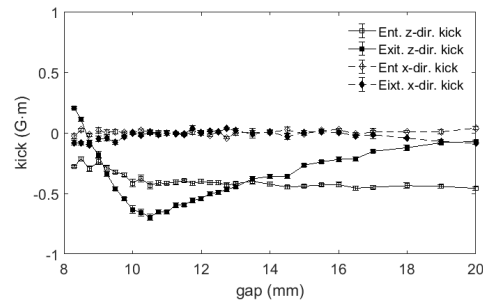


Figure 14: Measured end kicks.

SUMMARY

One additional undulator for the PAL-XFEL hard X-ray beamline was refurbished by using the prototype undulator frame. A new magnet block sorting was tried. The phase error seems mainly come from the magnet structure deformation. The surface roughness of the magnet structure and the magnet sorting may have a minor contribution to the phase error.

Content from this work may be used under the terms of the CC BY 3.0 licence (© 2019). Any distribution of this work must maintain attribution to the author(s), title of the work, publisher, and DOI

REFERENCES

- [1] I. S. Ko *et al.*, “Construction and Commissioning of PAL-XFEL Facility”, *Appl. Sci.* vol. 7, no. 5, p. 479, 2017, DOI: 10.3390/app7050479.
- [2] H.-S. Kang *et al.*, “Hard X-ray free-electron laser with femtosecond-scale timing jitter”, *Nature Photonics* vol. 11, p. 708, 2017, DOI:10.1038/s41566-017-0029-8.
- [3] D. E. Kim *et al.*, “Undulator commissioning experience at PAL-XFEL”, in *Proc. IPAC’17*, Copenhagen, Denmark, May 2017, paper TUPAB087, pp. 1520–1522, DOI:10.18429/JACoW-IPAC2017-TUPAB087.
- [4] F.-J. Börgermann, “Improvements In Production of Permanent Magnets and Pole-Pieces for Undulators”, in *Proc. IPAC’17*, Copenhagen, Denmark, May 2017, paper TUPAB041, pp. 1415–1417, DOI:10.18429/JACoW-IPAC2017-TUPAB041.